

Pulse Compression by Difference-Frequency Generation with Engineered Aperiodic Optical Superlattice

Yan KONG, Xianfeng CHEN,* Pinchuan LI and Yuxing XIA

Department of Physics, the State Key Laboratory on Fiber Optic Local Area Communication Networks and Advanced Optical Communication Systems, Shanghai Jiao Tong University, 800 Dong Chuan Road, Shanghai 200240, China

(Received 18 September 2006)

We theoretically propose a procedure for designing quasi-phase-matching (QPM) gratings for compressing ultrashort optical pulses during difference-frequency generation. The grating consists of blocks of crystal with the same block length and the direction of spontaneous polarization of each block is determined by an optimal algorithm through which the sign of the nonlinear coefficient of each block is optimized to make the phase response of the grating the same for different wavelengths of the output idler waves so that the generated idler pulse from the end of the crystal will be compressed during difference-frequency generation. Pumped by a cw (or a quasi-cw) laser, the generated idler pulse is compressed beyond its Fourier-transform limit in the simulations.

PACS numbers: 42.65.Ky, 42.65.Re, 42.70.Mp

Keywords: Pulse compression, Difference-frequency generation(DFG), Ultrashort pulse, Fourier-transform limit

I. INTRODUCTION

Optical pulse compressing, used in many ultrafast laser systems, has become increasingly important since the development of chirped pulse amplification [1]. The utility of the linearly chirped gratings in quasi-phase-matching (QPM) for pulse compression and shaping by the second-harmonic generation (SHG) process has been demonstrated [1–7]. This technique relies on the engineerability of the QPM gratings and allows compressing of pulses at half the wavelength of the seed pulses. However, if it is desirable to obtain compressed pulses at wavelengths other than harmonic of the seed, the SHG process does not provide adequate flexibility.

In our earlier work, we described how an aperiodic quasi-phase-matching gratings design could be used to compress ultra-short optical pulses during second-harmonic generation [8]. In this paper, we extend this design to difference-frequency generation (DFG). In the DFG process, the wavelength of the generated idler pulse can be tuned just by employing a cw (quasi-cw) pump with a different wavelength. Thus, the femtosecond pulse from the Ti:Sapphire laser can be moved from 800 nm to other wavelengths.

QPM gratings generally use sign reversal of the nonlinear coefficient along the crystal length in a periodic or aperiodic fashion [9]; *i.e.*, mathematically, $d(z)$ is

a square wave whose amplitude is the intrinsic nonlinear coefficient of the material, d_{eff} . If the period and the duty-cycle modulation are assumed to be slow, $d(z)$ can be decomposed into the spatial Fourier components $d_m(z)$ with slowly varying amplitudes and phase:

$$d(z) = \sum_{m=-\infty}^{+\infty} d_m(z) = \sum_{m=-\infty}^{+\infty} |d_m(z)| \exp[iK_{0m}z + i\varphi_m(z)] \quad (1)$$

We define a kind of grating that consists of blocks of constant length of crystals whose spontaneous polarizations, *i.e.*, signs of the nonlinear coefficient, are arbitrary along the propagation direction. Compared with that of periodic domain inversion, this kind of structure can supply more reciprocal vector. By optimizing the domain structure, the generated idler waves have the same phase for different wavelengths. It is naturally expected that the DFG pulse can be compressed.

II. THEORETICAL INVESTIGATION

The frequency-domain envelopes, $\hat{A}_m(z, \Omega_m)$, are defined by [3]

$$\hat{E}_m(z, \omega) = \hat{A}_m(z, \Omega_m) \exp[-ik(\omega_m + \Omega_m)z], \quad (2)$$

*Corresponding Author: xfchen@sjtu.edu.cn

where the k vector is a function of frequency and $\Omega_m = \omega - \omega_m$ is the frequency detuning from the optical carrier angular frequency ω_m . This definition explicitly accounts for the effect of the interacting waves. These envelopes should not be confused with the conventional envelopes, $B_m(z, t)$, defined in the time domain; in this case, the Fourier transform of the electric field is expressed as

$$\hat{E}_m(z, \Omega_m) = \hat{B}_m(z, \Omega_m) \exp[-ik(\omega_m)z]. \quad (3)$$

We assume plane-wave interactions, the slowly varying envelop approximation, and the process of idler generation from the input signal and pump waves in the undepleted-pump and unamplified-signal approximation (here and in the rest of the paper, we use the subscript $m = i, s, p$ the denote the idle, the signal and the pump, respectively). In terms of these frequency-domain envelopes, we arrive at the following set of coupled equations from the Maxwell's equations in the frequency domain:

$$\begin{aligned} \frac{\partial}{\partial z} \hat{A}_i(z, \Omega_i) &= -i \frac{\mu_0 \omega_i^2}{2k_i} \hat{P}_{NL}(z, \Omega_i) \\ &\times \exp[ik(\omega_i + \Omega_i)]z, \end{aligned} \quad (4)$$

$$\frac{\partial}{\partial z} \hat{A}_s(z, \Omega_s) = 0, \quad (5)$$

$$\frac{\partial}{\partial z} \hat{A}_p(z, \Omega_p) = 0. \quad (6)$$

The nonlinear polarization is expressed as

$$\begin{aligned} \hat{P}_{NL}(z, \Omega) &= 2\epsilon_0 d(z) \int_{-\infty}^{+\infty} \hat{A}_s^*(z, -\Omega + \Omega') \hat{A}_p(z, \Omega') \\ &\times \exp\{i[k(\omega_s - \Omega + \Omega') - k(\omega_p + \Omega')]z\}, \end{aligned} \quad (7)$$

where we define $\Omega = \Omega_i = \omega - \omega_i$, $\Omega' = \omega' - \omega_p$ and use $\hat{A}_s^*(-\Omega) = \hat{A}_s^*(\Omega)$. From the Eq. (4) - Eq. (7), we obtain the signal, the pump and the output idler envelopes:

$$\hat{A}_s(z, \Omega) = \hat{A}_s(z=0, \Omega) = \hat{A}_s(\Omega), \quad (8)$$

$$\hat{A}_p(z, \Omega) = \hat{A}_p(z=0, \Omega) = \hat{A}_p(\Omega), \quad (9)$$

$$\begin{aligned} \hat{A}_i(L, \Omega) &= -i\gamma \int_0^L d(z) dz \int_{-\infty}^{+\infty} d\Omega' \hat{A}_s^*(\Omega' - \Omega) \\ &\times \hat{A}_p(\Omega') \exp[-i\Delta k(\Omega, \Omega')z], \end{aligned} \quad (10)$$

where $\gamma = 2\pi/(\lambda_i n_i)$, λ_i is the idle wavelength, and n_i is the refractive index at the idler frequency and the k -vector mismatch

$$\Delta k(\Omega, \Omega') = k(\omega_p + \Omega') - k(\omega_i + \Omega) - k(\omega_s + \Omega' - \Omega). \quad (11)$$

Now, we assume that the pump is a cw monochromatic wave; *i.e.*, its frequency-domain envelop is a delta function:

$$\hat{A}_p(\Omega) = E_p \delta(\Omega = 0), \quad (12)$$

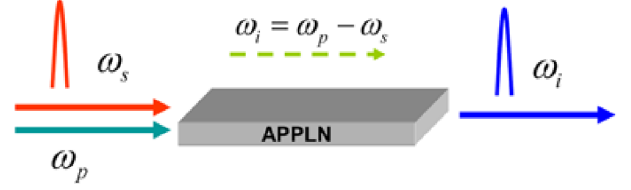


Fig. 1. Schematic of the pulse compression by DFG in aperiodically poled lithium niobate.

where E_p is the amplitude of the pump wave. Substituting Eq. (12) into Eq. (10), we obtain

$$\begin{aligned} \hat{A}_i(L, \Omega) &= -i\gamma \hat{A}_s^*(-\Omega) E_p \\ &\times \int_{-\infty}^{+\infty} d(z) \exp[-i\Delta k(\Omega)z] dz, \end{aligned} \quad (13)$$

where $\Delta k(\Omega)$ serves as the transform variable and is defined as

$$\Delta k(\Omega) = k(\omega_p) - k(\omega_i + \Omega) - k(\omega_s - \Omega). \quad (14)$$

III. NUMERICAL INVESTIGATION AND DISCUSSION

As Figure 1 show, a cw pump beam and a pre-chirped femtosecond pulse are launched in an aperiodically poled lithium niobate crystal. The generated idler pulse is compressed by adopting an appropriate domain-inverted structure.

We assumed a cw monochromatic pump wave with an optical carrier frequency ω_p (temporal peak), and on amplitude E_p , with its frequency-domain envelop being the same as the Eq. (12). Assuming a linearly chirped Gaussian signal pulse with an optical carrier frequency ω_s and a real (temporal peak) amplitude E_s , the time-domain envelope of the electric field that corresponds to this pulse is

$$B_s(0, t) = E_s \frac{\tau_0}{\sqrt{\tau_0^2 + iC_1}} \exp\left(-\frac{t^2}{2(\tau_0^2 + iC_1)}\right). \quad (15)$$

Using the frequency-domain envelope definition, we obtain $\hat{A}_s(\Omega)$ for this pulse as

$$\hat{A}_s(\Omega) = \frac{1}{\sqrt{2\pi}} E_s \tau_0 \exp\left[-\frac{1}{2}(\tau_0^2 + iC_1)\Omega^2\right]. \quad (16)$$

According to Eq. (13), $\hat{A}_i(\Omega)$ is determined by the modulated nonlinear coefficient, the crystal length L and the block number n . In our simulations, L and n are fixed, so our target tries to find the best distribution of signs of the nonlinear coefficient so that the generated idler pulse can be compressed. If the amplitude and the phase of the continue wave component, whose frequency varies among the spectra of the input signal pulses, are known, we will seek the optimal distribution of the nonlinear coefficient of the grating, whose phase response

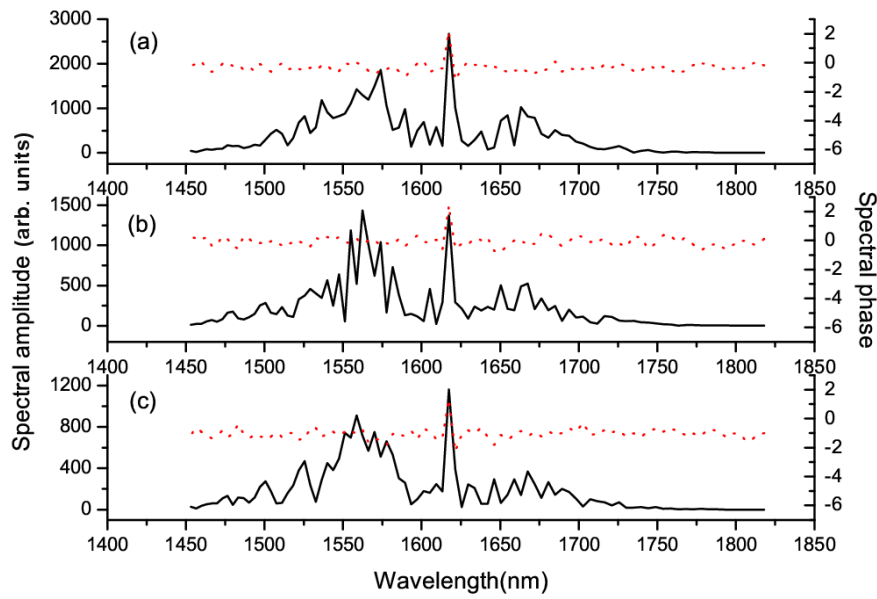


Fig. 2. (a), (b), (c) are the spectral amplitude (solid black line) and the spectral phase (dotted red line). The block lengths of the grating are $4 \mu\text{m}$, $5 \mu\text{m}$ and $8 \mu\text{m}$, respectively.

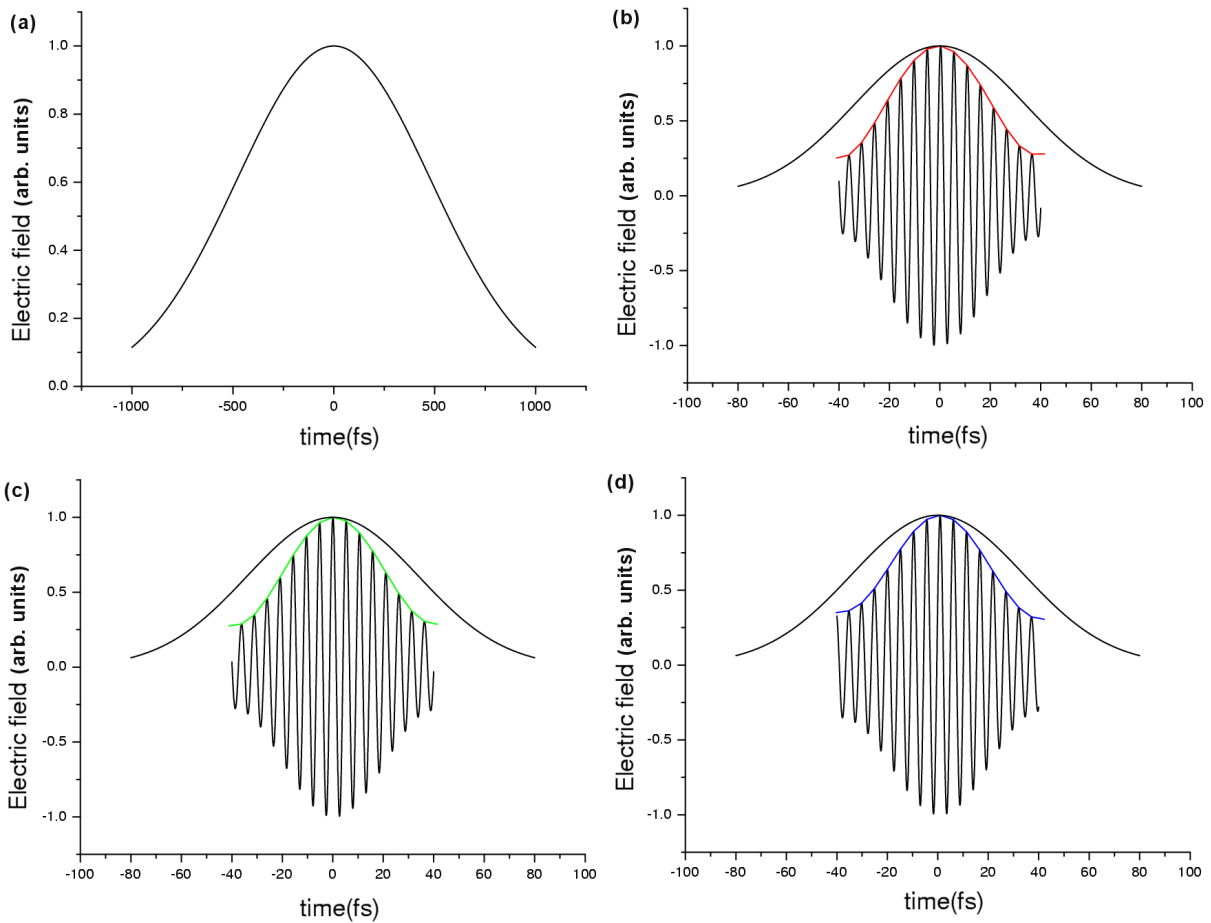


Fig. 3. (a) is the input linearly chirped pulse envelop, (b), (c) and (d) are the electric fields of the DFG and the Fourier-transform limit (FTL). The block lengths of grating are $4 \mu\text{m}$, $5 \mu\text{m}$ and $8 \mu\text{m}$, respectively. The pulse widths (FWHM) are 35.4 fs, 36.0 fs and 36.3 fs respectively.

is the same for all frequency components of the idler waves, which will lead to the output idler pulse being compressed.

In our calculations, an improved genetic algorithm- a cascading genetic algorithm- is employed to search for the best distribution of the signs of the nonlinear coefficient. In order to obtain a compressed idler pulse with a shorter pulse width, we should optimize the phase of the idler pulse, so we chose variance of the different phases as the objective function. The variance (which is the square of the standard deviation) can be described by the following equation:

$$\sigma^2 = \frac{1}{n}[(x_1 - \bar{x})^2 + (x_2 - \bar{x})^2 + \cdots + (x_n - \bar{x})^2]. \quad (17)$$

In the simulations, the parameters of the input signal pulse are $\tau_0 = 24.0$ fs (FWHM is 40.0 fs) and $C_1 = 20\tau_0^2$. The center wavelength of the signal pulse is 800 nm, the center wavelength of the pump pulse is 532 nm, the nonlinear optics crystal is lithium niobate and the temperature T is 25 °C. The refractive indices of lithium niobate for different wavelengths are calculated from the Sellmeier data of Ref. 10, the length of the grating L is 5 mm and the length of each block, l is chosen as 8 μm , 5 μm and 4 μm . $d(z)$ is optimized not only to make the phase response of the idler wave almost the same at the output, but also to make more frequencies meet the QPM condition.

Figure 2 shows the spectral amplitude and phase of the compressed idler pulse. After optimization of the domain inversion structure, the phase of the generated difference-frequency pulse becomes relatively uniform for wavelengths from 1453 nm to 1818 nm. The calculated results also indicate an efficiency increase with decreasing block length. On the assumption that the generated idler pulse is still Gaussian, the ideal full width at half maximum (FWHM) duration for the transform limit is calculated to be 56.6 fs at a wavelength of 1580 nm. In our results, the calculated idler pulse durations (FWHM) are 35.4 fs, 36.0 fs and 36.3 fs respectively, which are smaller than the theoretical value, as shown in Figure 3. Because the spectral amplitude is relative irregular, not a Gaussian distribution, the generated pulse can be even shorter than the Gaussian transform-limit. In addition, for a fixed block length l , the conversion efficiency is higher when the grating length is longer. The grating length L should be properly chosen by considering the converting efficiency and the group-velocity mismatch between the

signal pulse and the idler pulse.

IV. CONCLUSION

In conclusion, we have theoretically demonstrated a new procedure for designing a domain inversion grating that can compress the idler waves during difference-frequency generation. A cascading genetic algorithm is used to optimize the distribution of the nonlinear coefficient of each block to make the phase response the same for frequencies within the spectrum of the input pulse. In our simulation, the generated idler wave was successfully compressed beyond the Fourier-transform limit. Besides pulse compression, this method can also be used for pulse shaping.

ACKNOWLEDGMENTS

This research was supported by the National Natural Science Foundation of China (No. 60477016 and No. 10574092), the Foundation for Development of Science and Technology of Shanghai (No. 04DZ14001), and the ‘‘Shu-Guang’’ Scholar Plan of the Shanghai Education Committee.

REFERENCES

- [1] M. A. Arbore, O. Marco and M. M. Fejer, *Opt. Lett.* **22**, 865 (1997).
- [2] M. A. Arbore, *Opt. Lett.* **22**, 1341 (1997).
- [3] G. Imeshev, M. A. Arbore and M. M. fejer, *J. Opt. Soc. Am. B* **17**, 304 (2000).
- [4] G. Imeshev, M. A. Arbore, S. Kasriel and M. M. fejer, *J. Opt. Soc. Am. B* **17**, 1420 (2000).
- [5] P. Loza-Alvarez, M. Ebrahimpzadeh and W. Sibbet, *J. Opt. Soc. Am. B* **18**, 1212 (2001).
- [6] A. M. Schober, G. Imeshev and M. M. Fejer, *Opt. Lett.* **27**, 1129 (2002).
- [7] G. Imeshev, M. M. fejer, A. Galvanauskas and D. Harter, *J. Opt. Soc. Am. B* **18**, 534 (2001).
- [8] P. Li, X. Chen, Y. Chen and Y. Xia, *Optics Express* **13**, 6807 (2005).
- [9] X. chen, F. Wu, X. Zeng, Y. Chen, Y. Xia and Y. Chen, *Physical Review A* **69**, 013818 (2004).
- [10] D. H. Jundt, *Opt. Lett.* **22**, 1553 (1997).